Isotopic evidence for hydrologic change related to the westerlies in SW Patagonia, Chile, during the last millennium

Christopher M. Moy [a,*], Robert B. Dunbar [a], Patricio I. Moreno [b], Jean-Pierre Francois [b], Rodrigo Villa-Martínez [c], David M. Mucciarone [a], Thomas P. Guilderson [d], René D. Garreaud [e]

[a] Department of Geological and Environmental Sciences, 450 Serra Mall, Braun Hall (Building 320), Stanford University, Stanford, CA 94305-2115, USA
[b] Department of Ecological Sciences and Institute of Ecology and Biodiversity, Universidad de Chile, Las Palmeras 3425, Ñuñoa, Santiago, Chile
[c] Centro de Estudios del Cuaternario (CEQUA), Avenida Bulnes 01890, Punta Arenas, Chile
[d] Center for Accelerator Mass Spectrometry, Lawrence Livermore National Laboratory, P.O. Box 808, L-397 Livermore, CA 94550, USA
[e] Department of Geophysics, Universidad de Chile, Blanco Encalada 2002, Santiago, Chile

A B S T R A C T

The Southern Hemisphere westerly winds influence the spatial distribution of precipitation in southern South America and play a significant role in the global carbon cycle, yet little is known about how this important atmospheric circulation feature has varied in the past. Here, we present a sediment core record of late Holocene variability from Lago Guanaco, a small closed-basin lake located in Torres del Paine National Park, Chilean Patagonia. The park is located in the core of the modern wind field and variations in the intensity of the atmospheric circulation directly influence the hydrology of this region. We combine stable isotopic measurements of biogenic carbonate and bulk organic matter to identify two periods of increased evaporation between 900–550 and ~400–50 calendar years before present (cal yr BP). The first interval is coincident with the Medieval Climate Anomaly (MCA) while the more recent period is broadly coincident with the timing of the Little Ice Age (LIA). During the LIA interval, we observe simultaneous monotonic increases in the $\delta^{18}O$ of biogenic carbonate and *Nothofagus dombeyi*-type pollen, which we interpret as indicative of significant changes in the intensity of the southern westerlies during the last millennium. The isotopic and palynological variations in the Guanaco record are coincident with geochemical variations found in an Antarctic ice core record from Siple Dome, suggesting that the signal preserved in Lago Guanaco is regional rather than local, and that the LIA intensification was accompanied by a poleward shift in the southern margin of the westerlies. In addition, we interpret four periods of increased lake productivity centered on 900, 650, 500, and 200 cal yr BP from simultaneous increases in the $\delta^{13}C$ of bulk organic material and biogenic carbonate. These increases in lake productivity are most likely tied to increases in summer temperatures.

1. Introduction

The southern westerly winds are an important feature of atmospheric circulation in the mid- to high-latitudes of the Southern Hemisphere. Not only do the westerlies influence the amount and distribution of precipitation in South America and the other southern continents, the westerlies play a major role in carbon cycling in the Southern Ocean through their influence on air–sea gas exchange. Past changes in the latitudinal position of the westerlies are thought to influence the partitioning of CO_2 between the deep ocean and the atmosphere on glacial–interglacial timescales (Sigman and Boyle, 2000; Toggweiler et al., 2006). Furthermore, 20th century observations of increased westerly wind field strength have been shown to reduce the efficiency of the CO_2 sink in the Southern Ocean (Le Quere et al., 2007). Despite this recent interest in the southern westerly winds, there are significant gaps in our understanding of how the strength and the latitudinal position of the westerlies have varied in the most recent past. In the context of the last millennium, it is unclear how the intensity and position of the westerlies changed during important climate intervals like the Little Ice Age (LIA) and Medieval Climate Anomaly (MCA).

There are very few paleoclimate records that can directly address the question of how the westerlies have changed during short-climate intervals like the LIA and MCA. To date, such records from southern South America have been derived from locations

* Corresponding author. Tel.: +1 650 380 0395; fax: +1 650 725 0979.
E-mail addresses: moyc@stanford.edu (C.M. Moy), dunbar@stanford.edu (R.B. Dunbar), pimoreno@uchile.cl (P.I. Moreno), geofrancois@gmail.com (J.-P. Francois), rodrigo.villa@umag.cl (R. Villa-Martínez), tguilderson@llnl.gov (T.P. Guilderson), rgarreau@dgf.uchile.cl (R.D. Garreaud).

having indirect or convoluted relationship to the westerly wind regime, from discontinuous archives with insufficient resolution or length, and from paleoclimate proxies that are potentially equivocal and susceptible to multiple interpretations. Because of the challenges inherent in reconstructing westerly wind variability from such records, many critical questions remain unanswered. We identified three fundamental questions, which we will attempt to answer in this and forthcoming articles: What are the key forcing mechanisms that drive changes in the westerly wind field over the last millennium? Across this critical interval, what is the timing and direction of westerly wind variability? How did the vegetation and hydrologic balance of the region change in response to different westerly wind regimes? Understanding how the westerlies have varied during the last millennium is of particular importance, because it provides a baseline upon which to gauge both present and predicted change.

Southern South America is ideally suited for studies of past variability in the intensity and latitudinal position of the westerlies because it is the only landmass that is situated in the core of the wind field. In addition, several factors contribute to the significant relationship between precipitation and the intensity of zonal atmospheric flow. Extratropical precipitation is largely produced by frontal systems associated with surface depressions, whose growth is directly linked with the strength of the zonal flow aloft. Furthermore, surface depressions moving eastward are "steered" by the 700 hPa winds along the storm tracks (e.g., Trenberth, 1991), so stronger westerlies at interannual and longer time scales are conducive of a rapid growth and rapid succession of extratropical storms, leading to an increase in precipitation (Garreaud, 2007). Upstream of the Andes, orographic precipitation is an important source of moisture and its magnitude also increases with stronger westerlies; further downstream of the Andes, in contrast, downslope subsidence has a drying effect, so stronger westerlies can produce less precipitation there. In addition to precipitation, evaporation caused by increasing wind velocities also plays an important role in controlling the water balance in the semi-arid regions directly east of the Andes. Therefore, in SW Patagonia, the link between precipitation and hemispheric circulation is especially strong, providing a unique opportunity for evaluating past changes in the westerlies through reconstructing past changes in water balance.

The relationship between wind and precipitation has been used by others to investigate Holocene paleoclimate in SW Patagonia. These studies have primarily relied on pollen and charcoal evidence (Huber and Markgraf, 2003; Villa-Martinez and Moreno, 2007), although tree-ring (Villalba et al., 2003) and glacial deposits (Mercer, 1970, 1982; Aniya, 1995; Glasser et al., 2004) have also been used. Detailed pollen records developed from locations proximal to the moisture sensitive forest-steppe ecotone in southern South America identify increases in forest taxa (*Nothofagus dombeyi* type) at the expense of steppe taxa beginning about 6800 cal yr BP (Villa-Martinez and Moreno, 2007) or 5000 cal yr BP (Huber et al., 2004), and culminating during the last millennium. The majority of these records, however, show little or no change in hydrologic balance during the late Holocene, especially during important climate intervals such as the LIA and the MCA.

Stable carbon and oxygen isotope ratios of both biogenic and authigenic carbonate phases derived from lake sediments offer an additional tool for the reconstruction of past variability in hydrologic balance (Talbot, 1990; Seltzer et al., 2000; Leng and Marshall, 2004). In closed-basin lacustrine settings, where the primary loss of water is through evaporation, enrichment of lake water ^{18}O, mediated by the preferential loss of ^{16}O to water vapor, can be used to evaluate changes in the evaporation/precipitation (E/P) ratio though time (Li and Ku, 1997). Although this method can provide information on past hydrologic regimes, the requisite occurrence and preservation of sufficient carbonate material is rare in the lakes of Chilean Patagonia.

Here, we present a multi-proxy record of environmental change from Lago Guanaco as a part of an on-going project investigating climate change related to the westerlies in SW Patagonia. Lago Guanaco is unique in that it preserves abundant biogenic carbonate (ostracodes, bivalves, and *Chara* calcite) suitable for stable isotope analysis. Here, we focus on the most recent 1200 years of the record and combine carbon and oxygen stable isotope analyses on the carbonate and organic phases of the lake sediment to investigate past changes in hydrologic balance related to the westerlies.

2. Study area

Lago Guanaco is a small alkaline lake located in Torres del Paine National Park (51°52′S/72°52′W/200 m a.s.l.) directly east of the southern margin of the South Patagonian Ice field (Fig. 1). The lake occupies a small bedrock depression and is surrounded by hills with sporadic outcrops of the Cerro Torro formation, which largely consists of Late Cretaceous mudstones and sandstones (Winn and Dott, 1979). There are no carbonates present in the drainage basin. The lake has a surface area of 0.13 km^2, a maximum depth of 16 m, and is located in a small drainage basin (0.6 km^2). No streams enter the lake and a narrow outlet, which is presently 1.5 m above the current lake level, drains water directly into Lago Sarmiento during periods of higher lake level (Fig. 1b). When the lake level is similar to today, the lake is hydrologically closed and the principal mechanism for water loss is evaporation. When the lake level is higher, water loss through drainage over the sill and evaporation are the principal mechanisms. Although difficult to quantify, we estimate that loss of lake water to groundwater is relatively low due to the low hydraulic conductivity of the glacial silts and till that immediately underlie the organic lake sediments.

Lago Guanaco is a moderately eutrophic lake that supports a high diversity of emergent and submerged macrophytes along the shoreline and in shallow portions of the lake. A rim of *Scirpus* and *Juncus* reeds surrounds the site and dominates at water depths less than 1.0 m, accompanied by an occurrence of *Chara* in the northern shallow areas of the lake. *Myriophyllum* becomes abundant at greater depths in the lake, and *Pediastrum* is found on the lake surface. In addition, 2–5 mm thick microbialite crusts of *Rivularia* sp. cover cobbles in shallow areas of the lake. Between two field seasons in January 2004 and January 2007, we observed a ~1 m drop in lake level and a concomitant expansion of macrophytes toward the center of the lake.

Average annual rainfall measured in Torres del Paine from 1983 to 2006 was 730 mm/year—a small amount compared with precipitation a few tens of kilometers west over the Ice fields—and the mean annual temperature between 1983 and 1993 was 7.5 °C (CONAF). Fig. 2 displays monthly averages of temperature, precipitation, and relative humidity measured at the Torres del Paine National Park headquarters near the northern edge of Lago Toro (CONAF), along with surface wind speed from the NCEP–NCAR reanalysis (Kalnay et al., 1996), and the $\delta^{18}O$ of precipitation from Punta Arenas and Coyhaique (IAEA/WMO, 2004). Summers (DJF) are characterized by higher temperatures and wind speeds, low relative humidity, and lower $\delta^{18}O_{precip}$ values. Summer precipitation averages ~60 mm/month, which is only half of the estimated evaporation rate (~120 mm/month); peak precipitation values of ~80 mm/month are reached during late summer/early fall (March and April). In contrast, the winter months (JJA) are characterized by high relative humidity, low

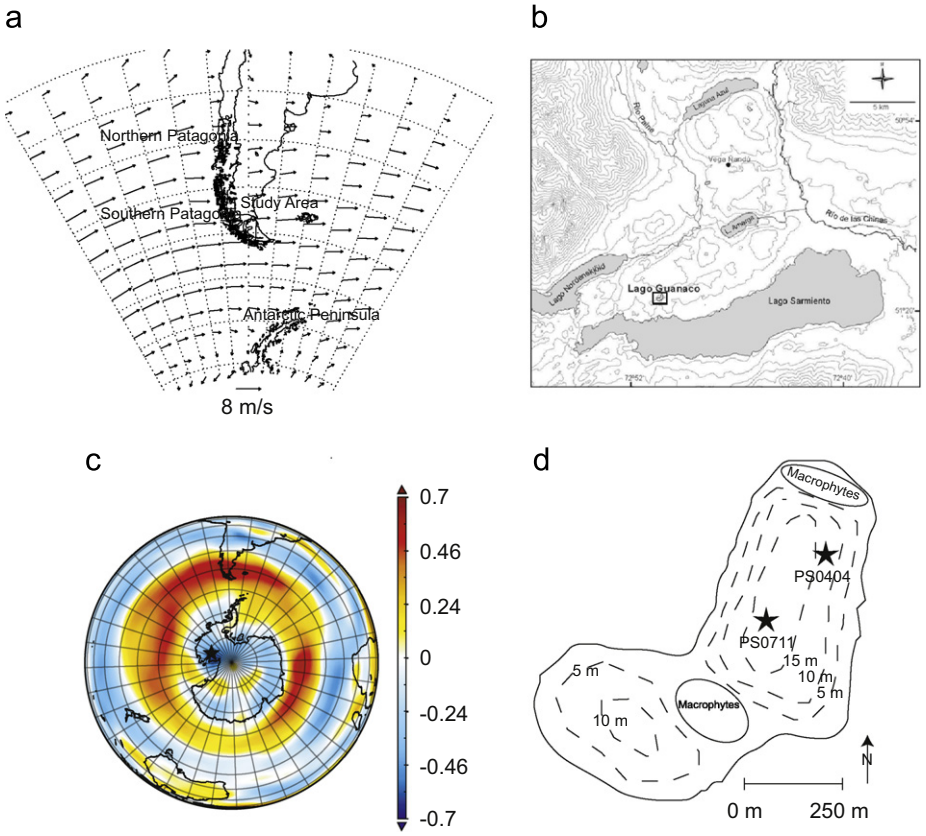

Fig. 1. (a) Annual average 700 hPa wind vectors from NCEP–NCAP reanalysis (Kalnay et al., 1996) illustrating wind direction and velocity for southern South America, the Southern Ocean, and the Antarctic Peninsula. The black rectangle surrounds the approximate study area shown in (b). (b) Eastern portion of Torres del Paine showing location of Lago Guanaco. (c) Annual correlation (r) of Torres del Paine precipitation and 700 hPa zonal wind. Precipitation measured in the park is directly related to the Southern Hemisphere westerlies over the Southern Ocean. (d) Generalized bathymetric map of Lago Guanaco with locations of coring sites. Star denotes location of Siple Dome.

wind speed, lower precipitation, and more negative values of $\delta^{18}O_{precip}$. Evaporation is also at a minimum and below the precipitation rate.

From these annual cycles, it is evident that seasonal variations of the large-scale winds (as derived from the NCEP–NCAR reanalysis data) significantly modulate the corresponding variations in precipitation and evaporation. On longer, annually averaged timescales, there is also a strong positive relationship between NCEP–NCAR reanalysis zonal wind in the Southern Hemisphere and the amount of precipitation falling in Torres del Paine (Fig. 1). Years with higher precipitation correspond to stronger zonal flow at 700 hPa over the entire Southern Hemisphere. The correlation is stronger during DJF, when the westerlies are strongest and located at their most poleward position. The interaction between the Andes and atmospheric circulation is complex and produces important heterogeneities in precipitation amount and seasonality on the eastern side of the Andes. Furthermore, there is a high degree of uncertainty regarding the spatial relationship between wind and precipitation due to the lack of long and continuous meteorological records in southern Patagonia. However, it appears that in the Torres del Paine region, precipitation and wind are well-coupled and reflect variations that are consistent with sites on the western Andean front (Schneider et al., 2003).

3. Methods

We collected undisturbed sediment-water interface cores from Lago Guanaco with a 7.5 cm diameter, 1-m long Plexiglass piston corer from two locations within the lake. Core PS0404SC was collected in January 2004 in 12 m water depth and is 67 cm long. Core PS0711SC is 97 cm long and was collected from the deepest basin in the center of the lake at 16 m water depth in January 2007 (Fig. 1d). PS0711SC contains the youngest tephra erupted from Volcán Reclús, a volcano that has been active throughout the late Quaternary (Stern, 2008) and is located ~60 km to the west of Lago Guanaco. We sampled both short cores in the field at 1 cm resolution. During January 2007, we measured pH, conductivity, temperature, and dissolved O_2 with a WTW 3500i multi-parameter water meter at depths of 0, 1, 2, 3, 6, and 12 m in the water column. We also collected water samples in 30 ml serum bottles to analyze both $\delta^{13}C$ of the total dissolved inorganic carbon (TDIC), and $\delta^{18}O$ and δD of the lake water at the surface and at depths of 6 and 12 m at the PS0711SC coring site. Samples for the analysis of $\delta^{13}C$ of TDIC were immediately poisoned with $HgCl_2$ to prevent biologic activity. Three additional surface water samples for the analysis of $\delta^{18}O$ and δD were collected from Lago Guanaco during February, March, and April 2007.

Sediment samples obtained from PS0404SC and PS0711SC were dried at 60 °C, crushed and loaded into silver capsules for bulk elemental and isotopic (C and N) analyses. Prior to analysis, sediment samples were acidified with a 6% sulfurous acid solution to remove carbonates (Verardo et al., 1990). Because acidification can preferentially remove some of the more labile N components and therefore introduce an analytical bias, bulk sediment samples for $\delta^{15}N$ were run without acid treatment in tin capsules. Samples of aquatic plants and terrestrial organic material used to evaluate potential sources of organic material were analyzed following similar procedures. All samples were analyzed at the Stanford

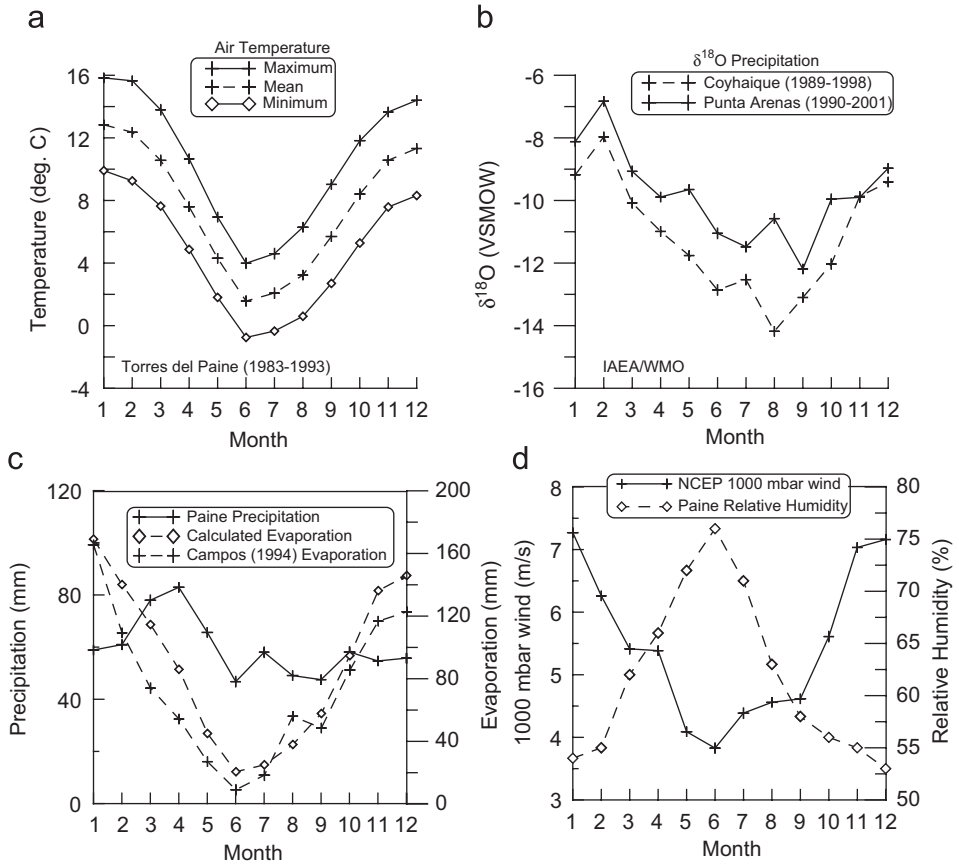

Fig. 2. Monthly climatologies of temperature, isotopic composition of rainfall, precipitation, evaporation, wind speed and relative humidity. (a) Monthly averaged minimum, maximum, and mean temperatures recorded in Torres del Paine from 1983 to 1993 (CONAF). (b) Weighted monthly averages of the $\delta^{18}O$ of precipitation recorded in Punta Arenas and Coyhaique, Chile (IAEA/WMO). Based on the latitude and topography of the study area, precipitation falling in the park should fall between these two lines. (c) Average monthly precipitation in Torres del Paine (CONAF) and calculated values of evaporation obtained from a modified Penman Equation (Linacre, 1992) and evaporation estimates presented in Campos et al. (1994). (d) Average monthly 1000 mb zonal wind (NCEP) and relative humidity (CONAF).

University Stable Isotope Laboratory using a Carlo Erba NA1500 Series 2 elemental analyzer coupled to a Finnigan Delta Plus isotope ratio mass spectrometer via a Finnigan Conflo II open split interface. Results are presented in standard delta notation with $\delta^{13}C$ reported relative to the VPDB carbonate standard and $\delta^{15}N$ relative to air. One standard deviation for replicate samples was 0.05‰ for $\delta^{13}C$, 0.14% for wt% TOC, 0.20‰ for $\delta^{15}N$, and 0.01% for wt% TN.

Bivalves and ostracodes were extracted from the bulk sediment of PS0404SC at 1 cm resolution by wet-sieving at 150 μm and oven drying the residue overnight at 60 °C. Each bivalve sample consists of 2–3 *Pisidium* sp. specimens individually selected, cleaned of surface contamination with deionized water, and homogenized with an agate mortar and pestle prior to analysis for isotopic composition (by mass spectrometry) and mineralogy (by X-ray diffraction (XRD)). Corroded shells were avoided and no overgrowths were observed during microscopic inspection. Adult *Candona* sp. ostracodes were also picked from the >150 μm fraction. Sediment adhering to the carapace was removed with a fine brush and 6–8 ostracodes of a narrow size fraction (0.75–1.0 mm) were run for isotopic analysis from each depth horizon.

In addition to bivalves and ostracodes, we analyzed the carbon and oxygen isotopic composition of the fine-fraction (<63 μm) sediment. Approximately 2 cm^3 of sediment was obtained from core PS0711SC at 1 cm intervals and wet-sieved through a 63 μm mesh. Following a method outlined in Ito (2001), the fine-fraction was bleached for 24 h using a 3% solution of sodium hypochlorite (NaClO), centrifuged and rinsed three times, before oven drying at 40 °C for 24 h.

Shell and fine-fraction carbonate was reacted with anhydrous phosphoric acid at 70 °C in a Finnigan Kiel III carbonate device interfaced to a Finnigan MAT 252 isotope ratio mass spectrometer at the Stanford University Stable Isotope Laboratory. Results are presented in standard delta notation with $\delta^{13}C$ and $\delta^{18}O$ reported relative to the VPDB standard. One standard deviation for replicates averaged 0.3‰ for both ostracodes and bivalves for $\delta^{13}C$ and $\delta^{18}O$. Standard deviation of the NBS-19 isotopic reference material analyzed with each suite of samples describes the instrumental precision and is 0.03‰ for $\delta^{13}C$ and 0.06‰ for $\delta^{18}O$. XRD analyses indicate that the bivalve shells are composed of aragonite and the fine-fraction is composed of calcite with no evidence of aragonite. Although not analyzed by XRD, ostracodes carapaces are composed of low-Mg calcite (Ito, 2001).

The $\delta^{13}C$ of the TDIC was analyzed following a procedure outlined in Appendix A of Gruber et al. (1999) at the Stanford University Stable Isotope Laboratory. Following this method, 15 ml of lake water was injected into a He gas sparger containing 2 ml of 12% H_3PO_4 for 10 min. The evolved gas passed through a dry-ice–alcohol–water trap followed by a liquid nitrogen cold trap, before samples were flame sealed in glass ampoules. The evolved and purified CO_2 was then measured on the Finnigan MAT 252 isotope ratio mass spectrometer. The $\delta^{18}O$ and δD of the lake water was analyzed at the Center for Stable Isotope Biogeochemistry at the University of California at Berkeley using a Gas bench and H/Device connected to a Thermo Delta Plus XL isotope ratio mass

spectrometer. The average standard deviation of the in-house standard analyzed with each suite of samples was 0.06‰ for $\delta^{18}O$ and 0.50‰ for δD.

To investigate changes in the deposition of calcium carbonate in the lake we analyzed the $<63\,\mu m$ fraction every 2 cm on the PS0711SC core using a UIC CM5240 automated acidification module connected to a UIC CM5014 coulometer. Weight percent biogenic silica (wt% BSi) was analyzed using a multi-step extraction method modified from Mortlock and Froelich (1989) and DeMaster (1981) every cm on the top 50 cm of the PS0404SC core. Standard deviations for wt% silica and carbonate replicates averaged 0.2 and 0.5 wt%, respectively.

An AMS radiocarbon chronology for the last ~1200 years was established using six dates on both bivalve carbonate and acid-base insoluble bulk organic material. Material for the dates was primarily obtained from PS0404SC and PS0711SC and analyzed at the Center for Accelerator Mass Spectrometry at Lawrence Livermore National Laboratory. In order to construct an age model that spanned the entire length of both short cores, we include two dates from the PS0711GT1 core, which is the first meter of sediment obtained with a modified Livingston square-rod corer taken from an anchored raft (Fig. 1d). We were able to successfully correlate the PS0711SC and PS0711GT1 cores based on the tephra derived from Volcán Reclús and the bulk organic isotope stratigraphy (Fig. 3). All ages have been corrected for isotope fractionation using $\delta^{13}C$ values determined on gas splits or residual processed bulk organic material. Radiocarbon dates were converted to calendar years BP (cal yr BP) with Calib 5.0.2 (Stuiver and Reimer, 1993) using the Southern Hemisphere calibration curve (McCormac et al., 2004). We used the median probability ages derived from Calib (Table 1) and applied a third-order polynomial to establish an age model for the cores. In addition, we created a composite age-depth model based on the longer PS0711SC core (Fig. 3). All of the dates from PS0404SC were transferred to the corresponding horizon in PS0711SC using the bulk organic elemental and isotope stratigraphy to determine tielines between the cores (Table 1).

4. Results

4.1. Lake chemistry

We measured the temperature profile of the lake in January 2007 and found it to be weakly stratified with surface waters 1.6 °C warmer than the bottom waters. Three days of unusually calm wind preceding the measurement likely allowed this stratification to occur, and a temperature profile obtained a week earlier from a ~20 m deep lake in the vicinity showed no stratification. The pH and conductivity of the lake during January 2007 was 8.6 and 515 μS/cm (0.3 PSU), respectively, and there was no variation of these parameters with depth (Table 2). The $\delta^{13}C$ of the TDIC averaged 3.92 ± 0.05‰ for measurements taken at the surface, 6 and 12 m water depth (Table 2). Similarly, the $\delta^{18}O$ and δD of the lake water showed insignificant variation with depth and averaged -4.24 ± 0.08‰ and -58.40 ± 0.57‰ for $\delta^{18}O$ and δD,

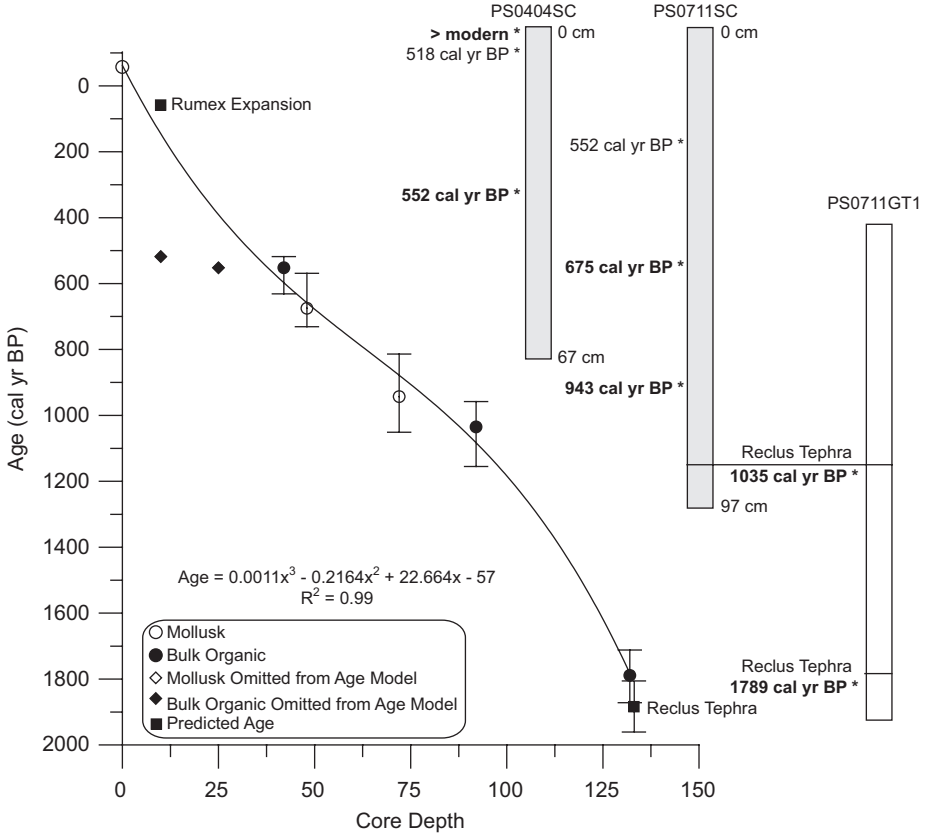

Fig. 3. Age-depth profile for Lago Guanaco cores PS0404SC and PS0711SC. We combined median probability ages obtained from all radiocarbon dates in addition to predicted ages for Rumex expansion and the late Holocene Reclus tephra and placed them on the depth scale of the longer PS0711 core. We use a third-order polynomial to interpolate between radiocarbon-dated intervals. Two dates were omitted from the age model based on the age obtained and stratigraphic position. The schematic shows the relative position of radiocarbon dates and how they relate to the longer PS0711GT1 core. Although we only present data from PS0404SC and PS0711SC (gray columns), we have included two dates from PS0711GT1 in order to extend our age model to the base of PS0711SC. Only bold ages have been included in the age model.

Table 1
AMS radiocarbon dates obtained from Lago Guanaco

No.	Lab code	Sample ID	Material	Original depth (cm)	Composite depth (cm)	$\delta^{13}C$ (PDB)	Core	Radiocarbon age	Median probability age	Lower 2σ	Upper 2σ
1	CAMS-107059	lgsc1_0	Mollusk	0	0	−4.84	PS0404SC	>modern ($D^{14}C = 177.8$)	−57	N/A	N/A
2	CAMS-115750	PS0404SC_34	Bulk organic	34	42	−27.69	PS0404SC	600+30	550	520	630
3	CAMS-131734	PS0711SC_48	Mollusk	48	48	−4.14	PS0711SC	775+40	680	570	730
4	CAMS-131735	PS0711SC_72	Mollusk	72	72	−4.77	PS0711SC	1080+35	940	810	1050
5	CAMS-133251	PS0711GT1_53	Bulk organic	93	93	−27.73	PS0711GT1	1185+45	1040	960	1170
6	CAMS-131264	PS0711GT1_90	Bulk organic	132	132	−27.26	PS0711GT1	1910+30	1790	1710	1870
Excluded ages											
7	CAMS-115749	PS0404SC_7	Bulk organic	7	10	−28.81	PS0404SC	520+30	520	500	540
8	CAMS-131733	PS0711SC_25	Mollusk	25	25	−3.87	PS0711SC	600+35	550	470	590

All radiocarbon dates were calibrated with Calib 5.0.2 (Stuiver and Reimer, 1993) using the Southern Hemisphere calibration curve (McCormac et al., 2004). We applied a third-order polynomial to the median probability ages to construct an age model for the cores.

Table 2
Water column properties and chemistry for Lago Guanaco during 2007

Water depth (m)	pH	Temperature (°C)	Conductivity (μS/cm)	Oxygen concentration (mg/l)	% O_2 saturation	$\delta^{13}C$ DIC (PDB)	$\delta^{18}O$ (VSMOW)	δD (VSMOW)
Water column measurements (January 2007)								
0	8.65	15	514	9.9	99.3	−3.85	−4.24	−58.52
1	8.61	15.5	517	9.8	97.9			
2	8.61	14.7	516	9.4	94.5			
3	8.61	13.3	515	9.3	94.7			
6	8.60	13.2	516	8.6	92.6	−3.93	−4.24	−58.06
12.4	8.60	13.5	515	8.2	82.4	−3.96	−4.26	−58.49

Date	$\delta^{18}O$ (VSMOW)	δD (VSMOW)
Guanaco surface measurements		
10 February 2007	−4.06	−57.25
28 March 2007	−3.81	−55.94
11 April 2007	−3.77	−55.47
Date	$\delta^{18}O$ (VSMOW)	δD (VSMOW)
Torres del Paine well water measurements		
13 April 2007	−13.94	−108.66
13 April 2007	−13.94	−110.13

respectively (Table 2). Three additional samples taken during the months of February, March, and April, reveal a slight increase of 0.48‰ and 2.93‰ for $\delta^{18}O$ and δD (Table 2) from February to April. Two groundwater samples obtained from a well located 5 km to the east of Guanaco in April 2007 average −13.9‰ and −109.4‰ for $\delta^{18}O$ and δD (Table 2).

4.2. Radiocarbon dates/age model

We use six AMS radiocarbon dates to establish a sediment chronology for the last 1200 years (Table 1; Fig. 3). A modern age was obtained from a bivalve at the sediment-water interface (PS0404SC), indicating that presently there is little or no contamination from old or dead carbon sources.

Our chronology accurately describes sedimentation in the lake during the late Holocene and compares well with regional paleoclimate studies. In order to provide an error estimate for our chronology during the last 1200 years, we use two chronological markers that can be compared to either regional historical accounts or to a tephra that has been dated in other lakes in Torres del Paine. These predicted ages have been presented in our age-depth profile (Fig. 3), but were not incorporated into the age model. The interpolated age for the expansion of the exotic herb *Rumex acetosella* in our record largely coincides (within 75 years) with historical narratives that describe the beginning of large-scale disturbance by Europeans at the end of the 19th century in the park area (Martinic, 1964). Second, the Reclús tephra at the base of PS0711GT1 (Fig. 3) has been identified in sediment cores from Vega Nandú and Lago Margarita (Villa-Martinez and Moreno, 2007) in Torres del Paine. Combining

the AMS ^{14}C ages from bulk organic matter immediately below the Margarita and Guanaco tephras yields a mean pooled age of 2000 ± 64 ^{14}C yr BP. Based on these data, we estimate that our age model is accurate to ~75 years in the most recent interval of the record and less than 70 years at the base of the record. Two dates, one from a bivalve and the second from bulk organic material, were omitted as outliers from the age model as they are too old based on their position in the core (e.g., 7 cm = 525 ^{14}C yr BP). These older dates can be caused by a combination of bioturbation and sediment mixing in the flocculent material comprising the top of the short core.

4.3. Bulk organic, fine-fraction carbonate, and biogenic silica

Bulk organic, fine-fraction carbonate, and biogenic silica variations from PS0404SC and PS0711SC are presented in Fig. 4. Wt% C and N were measured on both cores and average 13.25% and 1.25%, respectively. The sharp decline in both wt% C and N at ~1100 cal yr BP corresponds to the Reclús tephra preserved at the base of the record. The agreement and co-variation of wt% C and N between the two coring sites is excellent.

Wt% $CaCO_3$ of the fine-fraction sediment ($<63\,\mu m$) was measured on PS0711SC and averages 12% throughout the length of the record (Fig. 4). Carbonate concentration is generally high centered at 850 cal yr BP and between 200 and 400 cal yr BP. Conversely, low carbonate concentrations are coincident with the deposition of the tephra and during 100-year intervals centered at 750, 500, and 150 cal yr BP (Fig. 4). Wt% BSi measurements on PS0404SC exhibit an upward trend toward higher percentages through the late Holocene. High-frequency variability in biogenic silica tends to correspond with changes in wt% $CaCO_3$. Low values at ~500 and 100 cal yr BP are evident in both proxies (Fig. 4), while higher amounts of wt% BSi and $CaCO_3$ occur between 400 and 200 cal yr BP.

There are significant offsets in C/N ratio between the two cores (Fig. 4). The C/N ratio from PS0404SC is consistently higher, especially between 1000–600 and 500–100 cal yr BP, than the deeper and more distal coring site (PS0711SC). C/N values increase abruptly after 550 cal yr BP and remain high until 100 cal yr BP, and then they decline toward the present and reach the lowest values in the record.

The δ^{13}C records from the two Lago Guanaco core sites display consistent variability and excellent covariation during the last 1200 years ($r^2 = 0.97$). There is a long-term monotonic decrease in δ^{13}C values beginning at the base of the record and continuing to the core top (Fig. 4). Superimposed on this trend are three intervals of high δ^{13}C values centered at 900, 500, and 225 cal yr BP. There is also a sharp decline of 1.5‰ during the last 150 years. The δ^{15}N of the bulk-unacidified sediment was measured on the PS0711SC core and averages 4.23‰ during the length of the record. Values remain close to average throughout the record with a minor shift towards more negative values between 600 and 200 cal yr BP. This excursion is coincident with the large increase observed in C/N.

4.4. Biogenic carbonate

Biogenic and fine-fraction δ^{18}O and δ^{13}C profiles are presented in Fig. 5 and compiled in a cross-plot in Fig. 6. Adult *Candona* sp. and *Pisidium* sp. were picked from PS0404SC. δ^{18}O of *Candona* sp. is 1.8‰ more positive on average relative to *Pisidium* sp., with average *Candona* sp. δ^{18}O and δ^{13}C values are −0.9‰ and −2.9‰, respectively, while the *Pisidium* sp. bivalves average −2.9‰ and −3.7‰ (Fig. 5). We observe some similarity in the long-term variations in δ^{18}O of the biogenic carbonate and identify two periods of more negative values centered at 1000 and 500 cal yr BP and two periods where more positive values are evident and centered at 800 and 300 cal yr BP.

The fine-fraction sediment δ^{18}O and δ^{13}C averages −5.2‰ and −1.1‰, respectively, and exhibits variations in δ^{18}O and δ^{13}C that are similar to those evident in the bivalves and ostracodes. The fine-fraction δ^{18}O is similar to the *Pisidium* δ^{18}O profile (Fig. 5), where there are higher δ^{18}O values centered on 800 and 300 cal yr BP and low δ^{18}O values centered on 1000 and 500 cal yr BP. In addition, fine-fraction δ^{13}C variability is similar to that observed in the *Candona* sp. δ^{13}C. Fig. 6 compiles all of the δ^{18}O and δ^{13}C data from carbonate species analyzed in this study, including modern *Chara*, *Rivularia*, and isotopic values for equilibrium calcite. Equilibrium calcite values were calculated using the δ^{13}C TDIC samples collected in January 2007 and the δ^{18}O of water collected between January and April 2007, and average lake water temperature measured in Lago Sarmiento during 2006. There is a clear difference between the isotopic

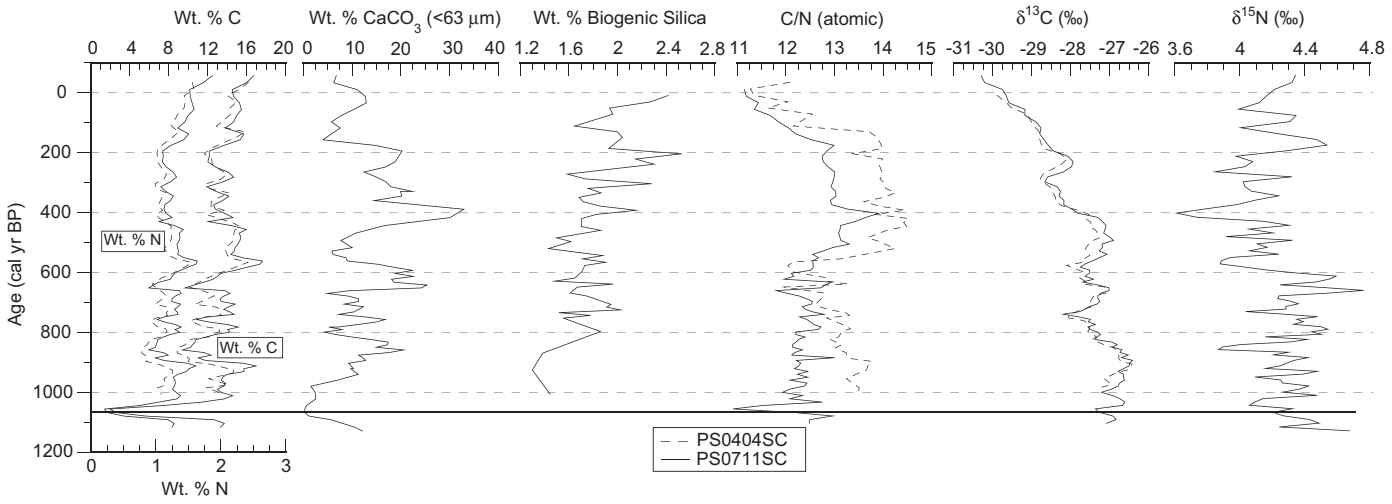

Fig. 4. PS0404SC and PS0711SC bulk organic isotopic and elemental concentrations, wt% $CaCO_3$, and wt% biogenic silica. The black horizontal line at the base of the plot refers to the Reclús Tephra exposed at the base of PS0711SC.

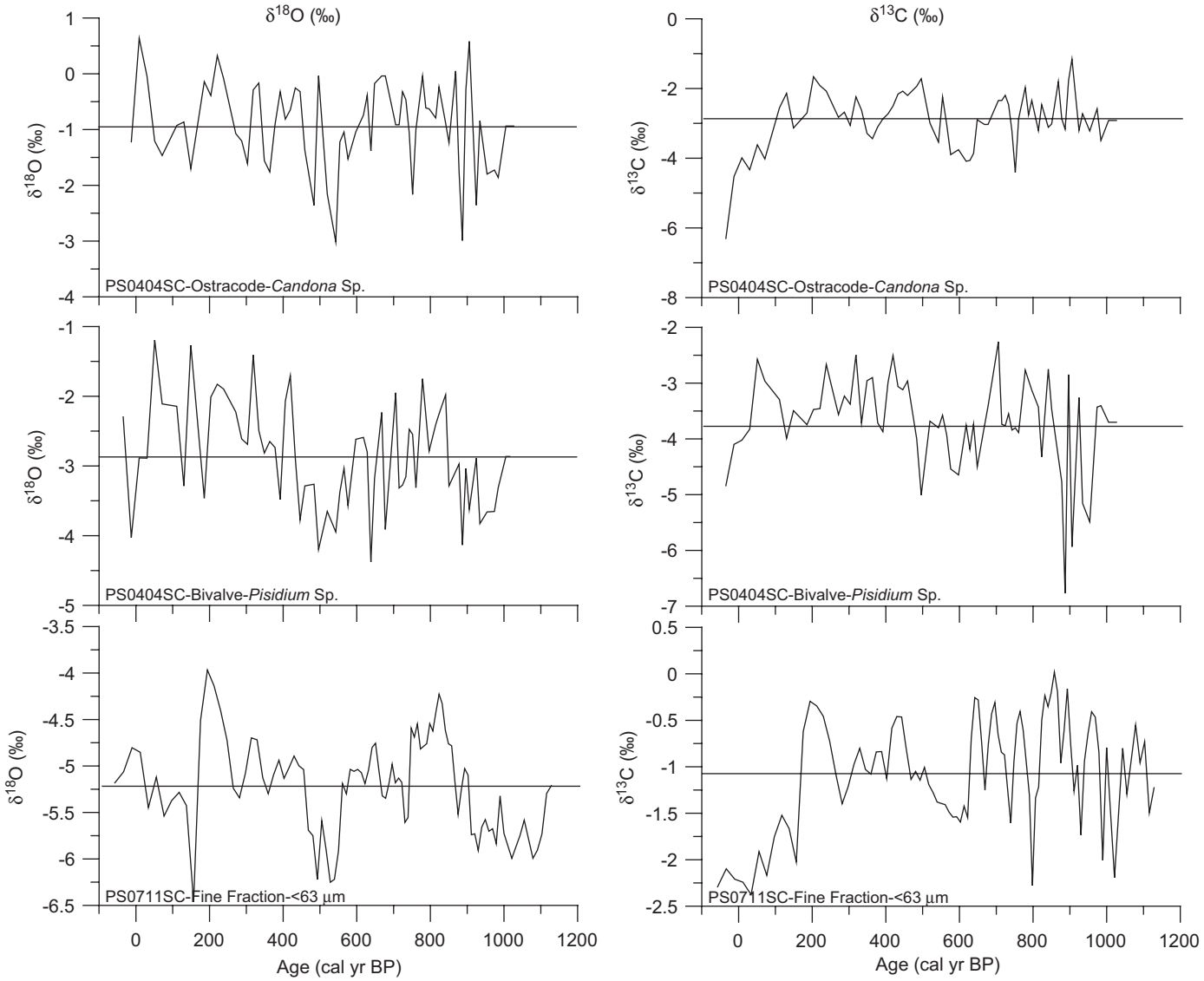

Fig. 5. Biogenic and fine-fraction sediment $\delta^{18}O$ and $\delta^{13}C$ profiles. The bivalve and ostracodes records were obtained from PS0404SC while the fine-fraction sediment was measured on the PS0711SC. Horizontal bars in each profile represent the average over the length of the record. The $\delta^{18}O$ records show consistent changes amongst the three carbonate phases while there is less co-variation observed in the $\delta^{13}C$ profiles.

values obtained from the biogenic carbonates versus those obtained from the fine-fraction sediment and modern *Chara*. The fine-fraction sediment plots in the same region as the modern *Chara* and is enriched in ^{13}C relative to equilibrium calcite by almost 2‰. Conversely, the *Candona* sp. plot in the range of the observed equilibrium values, while the *Pisidium* sp. plot at or up to 2‰ lower than observed equilibrium values (Fig. 6).

5. Discussion

5.1. $\delta^{13}C$-lake productivity

Understanding the possible sources of organic matter to the lake is important for the interpretation of bulk organic ($\delta^{13}C_{bulk}$ and $\delta^{15}N_{bulk}$) stable isotope ratios. C/N ratios are commonly used to evaluate the relative contributions of organic matter either produced within the lake (aquatic) versus those from terrestrial sources (Meyers, 2003). Because vascular land plants contain high amounts of cellulose, and algal sources do not, higher C/N values in lake sediments are commonly attributed to increased supply of terrestrial organic matter to the lake (Meyers, 1997). The contribution of aquatic macrophytes can also play a role in elevating the C/N ratio of lake sediment. C/N values for macrophytes living in Lago Guanaco have values ranging from 13 to 17, approaching the commonly ascribed value of >20 for terrestrial plants.

The C/N ratios presented here probably reflect a time-varying mixture of algal, aquatic plant, and terrestrial sources of organic material. C/N ratios decline gradually in core PS0404SC from 1000 to 600 cal yr BP before increasing abruptly at ~600 cal yr BP (Fig. 4). The increase in C/N is not the same in both cores. The PS0711SC core, which was collected from a deeper location farther from shore, displays a gradual upcore increase and does not attain the same high values as the shallow water core, indicating that less macrophytic or terrestrial organic material is reaching this location. C/N values decline gradually after 100 cal yr BP, suggesting a subsequent reduction in the input of external or macrophyte organic material. There are two ways that hydrographic changes can explain the increase in C/N ratio between 600 and

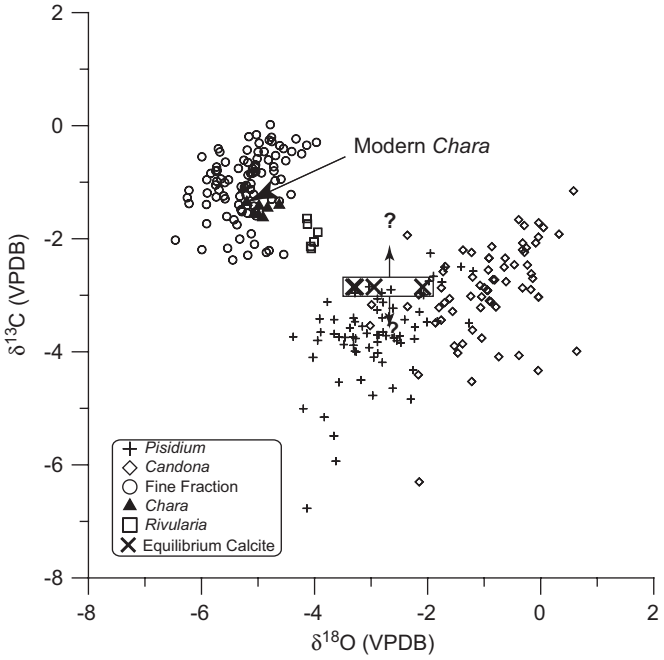

Fig. 6. Cross-plot of $\delta^{18}O$ and $\delta^{13}C$ values obtained from all of the carbonate sources measured in Lago Guanaco. The rectangle highlights equilibrium calcite values calculated using the $\delta^{18}O$ of surface waters collected in Lago Guanaco from January through April 2007, the average $\delta^{13}C$ TDIC obtained in January 2007, and water temperatures obtained from the Lago Sarmiento HOBO sensor for 2006. The arrows and question marks refer to the unknown seasonal range of $\delta^{13}C$ TDIC in Lago Guanaco. The modern *Chara* and fine-fraction sediment plot together indicating that the fine-fraction is most likely derived from *Chara* calcite. The fine-fraction and modern *Chara* is enriched in $\delta^{13}C$ by ~2‰ relative to the modern $\delta^{13}C$ of TDIC.

100 cal yr BP. Either increased run-off brings more terrestrial organic matter to the lake or lower lake level during this period promotes the growth of aquatic macrophytes close to the coring location. In additional to hydrologic change, high wind speeds can form waves that cause resuspension of littoral macrophytes and sediments and deposition in the center of the lake.

The *Candona* carapace and fine-fraction sediment can be used to better understand both the sources of organic matter and the carbon cycling/fractionation that takes place in the water column. Bivalve $\delta^{13}C$ is not considered here because it has been demonstrated that bivalves can incorporate up to 10% respired CO_2 while precipitating the shell and thus can exhibit values <2‰ lower than the isotopic composition of the TDIC (McConnaughey et al., 1997; Dettman et al., 1999; Lorrain et al., 2004). Bulk sedimentary $\delta^{13}C$ by itself responds to a number of different processes, including the sources of organic material being introduced to the lake, respiration, organic matter degradation, and changes in the lacustrine TDIC pool due to productivity and biologic uptake (Meyers and Teranes, 2002). On the other hand, carbonate $\delta^{13}C$ in the lake is largely controlled by CO_2 exchange between the atmosphere and the lake water as well as photosynthesis/respiration processes (Leng and Marshall, 2004). The $\delta^{13}C$ of ostracodes has been shown to reflect changes in the $\delta^{13}C$ of the TDIC pool of the lake (Schwalb et al., 2002) and adult *Candona* sp. have been shown to precipitate within 1‰ of the $\delta^{13}C$ of the TDIC (von Grafenstein et al., 1999).

The $\delta^{13}C$ of calcite in the fine-fraction should also track changes in the $\delta^{13}C$ of TDIC, but in this setting, will follow a different C pathway. Fig. 6 displays the relationship between $\delta^{13}C$ and $\delta^{18}O$ for all of the carbonate species analyzed in this study. The fine-fraction sediment and modern *Chara* plot together; both are enriched by ~2‰ in ^{13}C relative to *Candona* and the modern $\delta^{13}C$ of the TDIC. The relationship between the fine-fraction sediment and *Chara* indicates that calcite in the fine-fraction is largely formed in an alkaline zone proximal to the growing *Chara* stems, rather than precipitating in isotopic equilibrium. *Chara* is able to utilize HCO_3^- for photosynthesis and effectively discriminates against ^{13}C through the process of assimilation (McConnaughey, 1991; Hammarlund, 1997). Discrimination against ^{13}C by *Chara* leaves the surrounding aquatic environment proximal to the stem enriched in ^{13}C relative to the TDIC and the calcite precipitated in this zone exhibits more positive isotopic values.

Bulk organic $\delta^{13}C$ exhibits an overall decrease since 1200 cal yr BP. Superimposed upon the $\delta^{13}C_{bulk}$ trend are four periods of small (0.5–1.0‰) but significant $\delta^{13}C$ increases (Fig. 7). To investigate these short-period changes in the bulk $\delta^{13}C$, we detrended the series using singular spectrum analysis (Ghil et al., 2002). We reconstructed the leading empirical orthogonal function (EOF; the component that captures the majority of the low frequency trend), and then subtracted this component from the original series. Fig. 7 displays the original and the detrended bulk $\delta^{13}C$ time series along with the $\delta^{13}C$ profiles obtained from the fine-fraction sediment and *Candona* sp. The higher frequency variability in the detrended bulk organic series corresponds with simultaneous shifts observed in both ostracode and fine-fraction $\delta^{13}C$, indicating that bulk $\delta^{13}C$ is influenced by summertime changes in the DIC pool of the lake. Because the growth of *Chara* is restricted to the shallow littoral areas of the lake, it is likely that growth is restricted to the summer months when temperatures are optimal (Pentecost et al., 2006). The $\delta^{13}C$ variations highlighted in Fig. 7 are the result of increased summertime productivity in the lake, probably driven by increased summer temperatures.

We also observe a significant decrease in $\delta^{13}C$ in all four profiles during the last ~150 years. This reduction is probably related to the contribution of the Suess effect on the lake water DIC. The Suess effect is a ~1.4‰ reduction in the $\delta^{13}C$ of atmospheric CO_2 caused by burning of fossil fuels and has been identified in other lake systems (Schelske and Hodell, 1995; Brenner et al., 1999; O'Reilly et al., 2003). In addition to the Suess effect, input of soil DIC from land use changes (deforestation) could also contribute to the reduction in the $\delta^{13}C$ profiles presented here.

5.2. Hydrologic change

Changes in hydrologic balance in Lago Guanaco can be inferred using carbonate $\delta^{18}O$ data combined with wt% $CaCO_3$. $\delta^{18}O$ of the biogenic and fine-fraction carbonate is influenced by the isotopic composition of the lake water, temperature, and any species-specific disequilibrium or vital effects. The isotopic composition of the lake water, in turn, is a function of the isotopic composition of the inputs, which here include precipitation, groundwater, and surface runoff, and subsequent modification by evaporative processes and other outflow. In lakes, the use of specific carbonate fossils is advantageous because each group is composed of a single mineralogy, occupies the same habitat through time and is well characterized in a number of lacustrine environments (von Grafenstein et al., 1999). Interpretation of the Guanaco biogenic carbonate records is probably limited to the summer months, due to the different seasons of calcification. The adult *Candona* sp. calcifies during the late summer (von Grafenstein et al., 1999). The bivalves can live 3–5 years, but most likely they calcify only during the summer months when environmental conditions are conducive (Ito, 2001). Calcite derived from *Chara* is most likely formed when temperatures are highest in the middle to late summer (Pentecost et al., 2006).

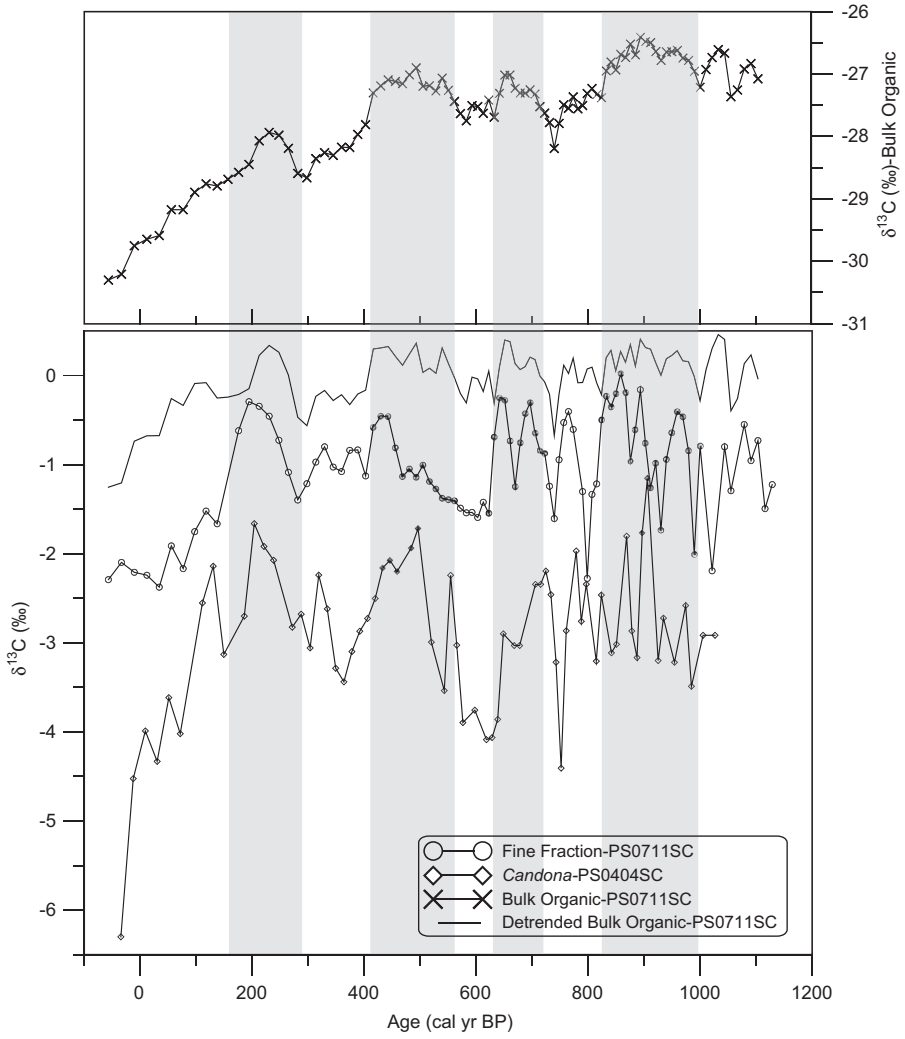

Fig. 7. Carbon isotope stratigraphy of the bulk organic, detrended bulk organic, fine-fraction, and *Candona* sp. highlighting consistent variations among the different profiles during the last 1200 years. The long-term trend in the bulk $\delta^{13}C$ was removed by subtracting the first EOF with singular spectrum analysis. The gray bars highlight intervals of increased lake productivity inferred from increases in $\delta^{13}C$.

The isotopic composition of precipitation ($\delta^{18}O_{precip}$) offers an important starting point for interpreting the Guanaco biogenic isotope records. Two IAEA/WMO stations in southern and central Patagonia have been collecting precipitation samples at monthly intervals for at least 10 years. The Coyhaique station is located 600 km to the north in central Patagonia east of the Andes and has continuous precipitation data from 1989 to 1999, while the Punta Arenas station is located 270 km to the south of the study area on the Strait of Magellan and has continuous data from 1990 to 2001. Fig. 2b shows the average monthly values for the isotopic composition from these two locations. Summer values (DJF) for precipitation average −8‰ for both stations while winter (JJA) values average −11‰ and −13‰ for Punta Arenas and Coyhaique, respectively. Based on the location and high topography to the west of Guanaco, the isotopic composition of precipitation from these two locations probably provides maximum values for Torres del Paine precipitation. Stern and Blisniuk (2002) investigated the interaction of topography and the isotopic composition of precipitation in central Patagonia by collecting surface water, groundwater and precipitation. They found that the Andes produced a 4‰ "rain shadow" effect. Precipitation samples collected from sites with similar topographic barriers to Guanaco (~2000 m) had annual precipitation values ranging from −13‰ to −16‰. Groundwater collected from springs in the central Patagonia region range from −11‰ to −15.5‰ (Stern and Blisniuk, 2002) and two samples from a well close to Lago Guanaco average −13.9‰.

The oxygen isotopic composition of freshwater bivalves have been shown to precipitate at or very close (within 1‰) to isotopic equilibrium of the lake water (Dettman et al., 1999; von Grafenstein et al., 1999). Despite $\delta^{18}O$ values for precipitation and groundwater ranging from −8‰ to −14‰ in the region, the average core-top $\delta^{18}O_{bv}$ value for PS0711SC collected in January 2007 is −3.7‰ and average summer $\delta^{18}O$ collected from the lake in 2007 is −4.05. The greater than 4‰ difference between the hydrologic inputs and the core top *Pisidium* indicates that there is significant evaporative enrichment of the modern lake water and downcore variations in $\delta^{18}O_{bv}$ primarily record changes in evaporative processes. Today the lake is hydrologically closed and the high $\delta^{18}O$ values are indicative of excess evaporation over precipitation. We identify three intervals of high $\delta^{18}O$ in *Pisidium* and the fine-fraction sediment between 950 and 750, 650 and 575, and 400 and 50 cal yr BP, which we interpret as periods of increased evaporation. There are also two pronounced periods of low $\delta^{18}O$ with values of −4.75‰ and −3‰, indicating less evaporative enrichment between 1100–1000 and 550–450 cal yr BP

(Fig. 6). During these times, it is possible that lake level was high enough to drain over the sill. In this state, equilibrium carbonate $\delta^{18}O$ values would approach the isotopic composition of rainfall and the system would approximate an 'open lake' (Leng and Marshall, 2004).

Wt% $CaCO_3$ of the fine-fraction ($<63\,\mu m$) sediment varies in a similar fashion as the $\delta^{18}O$ of the biogenic carbonate during the last 1200 cal yr BP (Fig. 8). As mentioned above, the fine-fraction carbonate is primarily derived from *Chara* calcite, which forms close to the stems in highly alkaline microenvironments. Higher sediment carbonate content could reflect lower lake levels driving the expansion of *Chara* towards the coring site, increases in summer temperature, or other ecological conditions that favor *Chara* production and photosynthesis. In addition, there may be a contributing component that is derived from equilibrium biogenic carbonate precipitation in the epilimnion of the lake during periods of high phytoplankton productivity. The contribution, however, must be small as fine-fraction sediment isotopic values do not approach those derived from *Candona* and *Pisidium* in the $\delta^{13}C$ and $\delta^{18}O$ cross-plot (Fig. 6), and high summer winds prohibits long-term thermal or chemical stratification of the lake water.

High wt% $CaCO_3$ coincident with high $\delta^{18}O$ biogenic carbonate values are centered at 600 cal yr BP and between 400 and 200 cal yr BP are most likely indicative of increased evaporation (Fig. 8). However, the more recent period is also associated with high C/N values (Fig. 4), indicating either lake levels declined and there was increased erosion of the littoral areas and influx of sediment with higher C/N values, or there was increased run-off and wind-induced resuspension of littoral sediments and macrophytes. Based on comparision with pollen records derived from the lake, we favor the latter explanation and will discuss this further below. Beginning at 1050 cal yr BP we observe an increase in *Pisidium* and fine-fraction $\delta^{18}O$ that culminates at ~800 cal yr BP. Wt% $CaCO_3$ follows the trend in $\delta^{18}O$, but abruptly declines for ~100 years at 800 cal yr BP. The divergence at 800 cal yr BP between the isotopic and wt% $CaCO_3$ is probably related to increasing salinities and/or changes in ecologic conditions that work towards limiting *Chara* production. Culture and observational studies have documented that *Chara* production and distribution is sensitive to increasing salinity (Wollheim and Lovvorn, 1996; Blindow et al., 2003). Increased salinity during enhanced evaporative conditions (as recorded by $\delta^{18}O$) may have

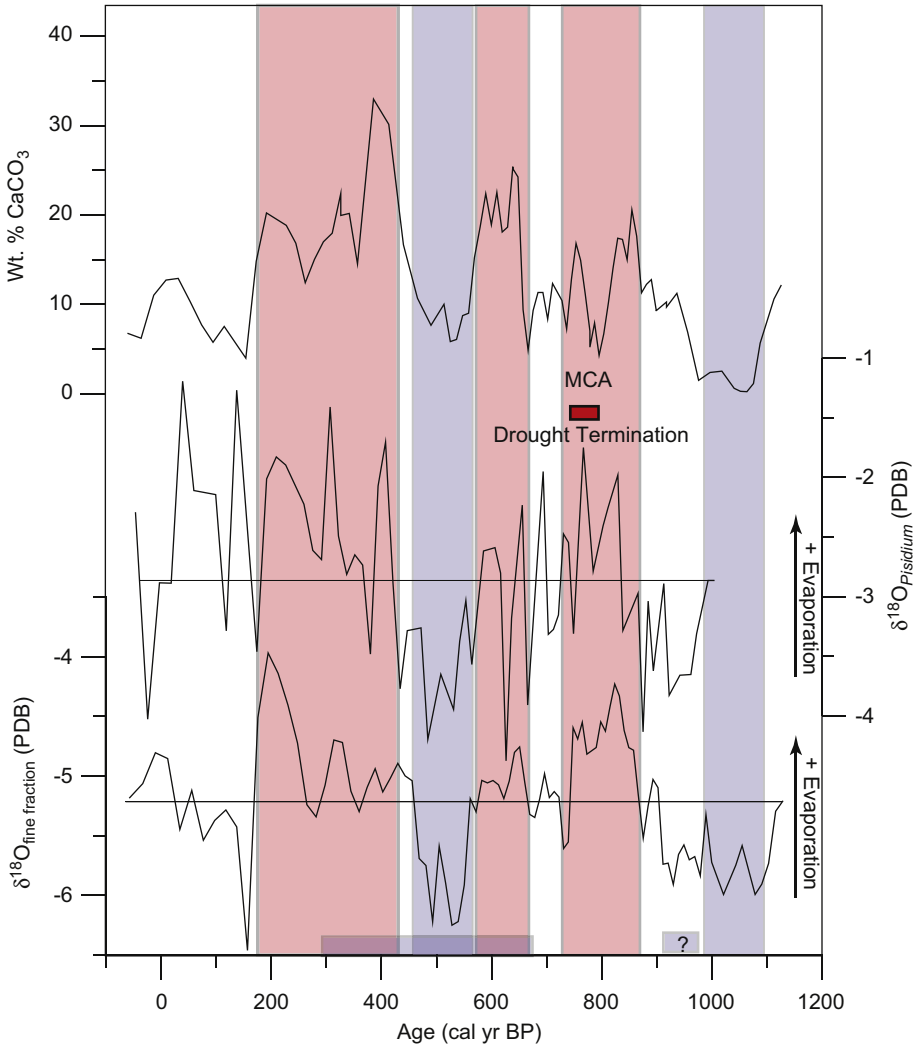

Fig. 8. Compilation of proxies illustrating hydrologic change in S Patagonia during the last ~1200 cal yr BP. The bottom two profiles display changes in evaporation interpreted from the $\delta^{18}O$ of fine-fraction sediment and *Pisidium* from Lago Guanaco. We identify three periods of enhanced evaporation (red bars) centered at 800, 650, and 300 cal yr BP and two periods of positive moisture balance centered at 1100 and 500 cal yr BP (blue bars). The rectangle at the base of the plot indicates a reconstructed cool and wet interval in N Patagonia from tree-rings (Villalba, 1994) and the red box corresponds to drought termination in central Patagonia inferred from radiocarbon-dated trees exposed in Patagonia lakes (Stine, 1994).

been an important mechanism for reducing sediment $CaCO_3$ concentrations at this time.

5.3. Medieval Climate Anomaly

There is evidence for increased aridity during the MCA in the Guanaco record. The first 100 years of the interval between 900 and 700 cal yr BP are characterized by higher *Pisidium* and fine-fraction sediment $\delta^{18}O$, and relatively high wt% $CaCO_3$ (Fig. 8). Peak $\delta^{18}O$ values are centered on 800 cal yr BP and are broadly coincident with the timing of drought termination in central Patagonia as reconstructed from radiocarbon dating of relict tree stumps submerged in locations proximal to Lago Cardiel and Lago Argentino (Stine, 1994). This period of time is also characterized by warmer summer temperatures as reconstructed from tree-ring records in northern Patagonia (Villalba, 1994).

5.4. Westerly wind variations

In Lago Guanaco, we have reconstructed changes in the forest-steppe ecotone during the last millennium by producing a paleovegetation index of *Nothofagus* to *Poaceae*. Because the ecotone is controlled by moisture availability, increases in the ratio reflect eastward expansion of the forest due to enhanced precipitation. In Fig. 9, we show the relationship between *Pisidium* $\delta^{18}O$ and a five-point running average of the paleovegetation index. *Pisidium* $\delta^{18}O_{bv}$ and the index evolve similarly during much of the last 500 years: as the index increases, so does the *Pisidium* $\delta^{18}O$. The co-variation of these two parameters is related to increasing wind intensity and moisture of westerly origin during the LIA.

Wind plays an important role in controlling evaporation in Torres del Paine. Calculated and observed evaporation rates from the park are highest during the summer months (150–175 mm/

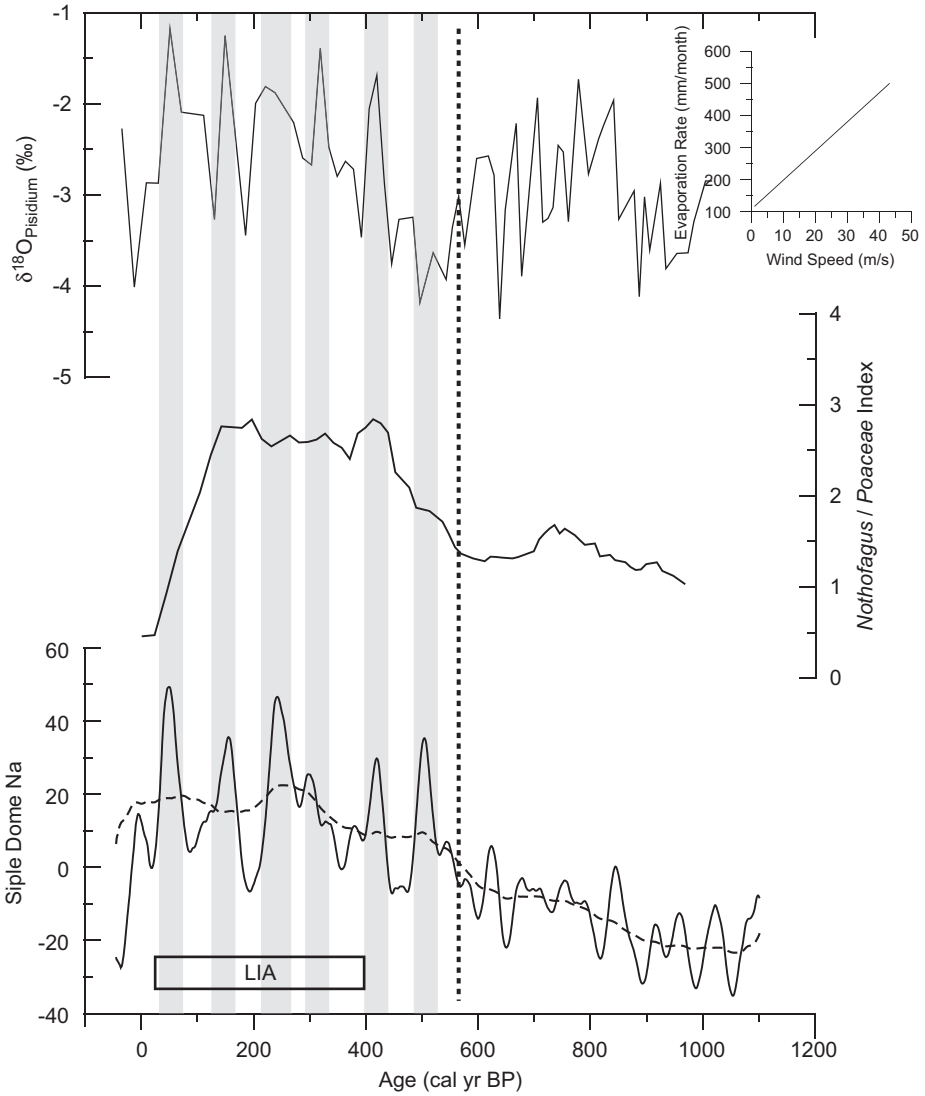

Fig. 9. Isotope and pollen evidence for increased westerly wind intensity during the LIA. Concomitant increases in *Pisidium* $\delta^{18}O$ and the *Nothofagus/Poaceae* ratio are indicative of increased wind, enhanced evaporative conditions, and increased precipitation during the last 500 years. Increased precipitation will drive an eastward expansion of the forest and enhance delivery of *Nothofagus* pollen to the lake, while increased winds will increase isotope fractionation through evaporative effects (see text). The inset diagram illustrates the relationship between evaporation rate and wind speed when temperature and relative humidity remain constant in a modified Penman equation (Linacre, 1992). The variations observed in the Guanaco record show a strong similarity to the first EOF of Na^+ concentration from Siple Dome, Antarctic (Kreutz et al., 1997) calculated using a 25- (solid line) and 115-year (dashed line) window. Kreutz et al. (1997) attribute increases in Na^+ concentrations during the last 500 years to deepening of the Amundsen Sea Low, which increases the delivery of sea salt to the ice core location. The vertical dashed line is the calculated break in slope that Kreutz et al. (1997) use to identify the start of the LIA. The paleovegetation declines at ~150 cal yr BP due to widespread clearance of the *Nothofagus* forest for livestock grazing.

month) due to the high wind speeds, low relative humidity, and relatively higher temperatures (Campos et al., 1994). Using a modified Penman equation for an evaporating lake, which incorporates wind speed, temperature, and dew point (calculated from relative humidity) (Linacre, 1992), we calculated monthly evaporation rates for a range of wind speeds keeping temperature and dew point constant (Fig. 9). Increasing wind speed from 20 to 30 m/s, which is within the range of summer wind velocities recorded in the park during the 1980s (Campos et al., 1994) would increase the evaporation rate by 40% (Fig. 9).

The seasonality of wind-driven changes is important for reconciling the isotopes and pollen data from the Lago Guanaco record. Increasing winds during the summer months (DJF) will increase both evaporation and precipitation, but during this season the E/P ratio is ~2 (Fig. 2). Strong winds during winter will also increase both evaporation and precipitation, however E/P is slightly below 1 during this season. When averaged over the year, the evaporation signal revealed by the isotope data should override precipitation and result in a negative water balance. Therefore, the trends observed in both the isotopes and the pollen index can be accounted for by an overall increase in wind intensity.

5.5. Little Ice Age

The LIA is generally thought to have occurred between 400 and 150 cal yr BP, although the exact timing and nature of this event is not globally consistent (Bradley et al., 2003). In Lago Guanaco, the LIA ushers in an interval of increased C/N, $\delta^{18}O$ of biogenic and fine-fraction sediment carbonate, and wt% $CaCO_3$, in addition to increases in the *Nothofagus*/*Poaceae* ratio (Figs. 8 and 9). Taken together, these data argue for an intensification of the westerlies, increased evaporation, and an eastward expansion of the forest driven by increased precipitation. The timing of changes presented here are similar to those observed in the Siple Dome ice core record from Antarctica. The concentration of sea salt in ice cores obtained from Siple Dome has been used as a proxy for atmospheric circulation around western Antarctica during the late Holocene (Kreutz et al., 1997). Kreutz et al. (1997) attribute variations in the intensity of the Amundsen Sea Low (ASL), situated directly west of the Antarctic Peninsula, drive changes in sea salt delivery to the coring site; a strengthened ASL allows for increased delivery of sea salt. During the second-half of the last millennium, there is a monotonic increase in the delivery of Na^+ beginning at ~550 cal yr BP, coincident with increasing *Nothofagus* percentages in the Lago Guanaco record (Fig. 9). To separate the long-term trends from the high-frequency variability in the record, we calculated the leading EOF of the Siple Dome Na^+ ion time series using singular spectrum analysis (Ghil et al., 2002). In Fig. 9, we present the first modes of variability calculated using 25- and 115-year window lengths to highlight the multi-decadal variability and long-term trends in the Siple Dome Na^+ record. We varied the window length from 10 to 200 years and found that the variability at 25 and 115 years, accurately captures the multi-decadal and the long-term trend, respectively. The Siple Dome Na^+ time series, as well as the paleovegetation ratio and *Pisidium* $\delta^{18}O$ from Guanaco, evolve similarly during the last 500 years. The Na^+ and the palynological ratio both trend towards higher values starting at ~550 cal yr BP, while the $\delta^{18}O$ of *Pisidium* lags initially and then responds. All three records exhibit sustained high values from 450 until ~150 cal yr BP, when the pollen profile begins to decline due to widespread clearance of the *Nothofagus* forest for livestock grazing (lower paleovegetation index values). Although it is interesting to highlight that the Guanaco *Pisidium* $\delta^{18}O$ and the Siple Dome record (25 year window) show consistent in-phase multi-decadal variations during the LIA, the uncertainty in our radiocarbon chronology precludes a direct assessment of this relationship.

The association between the Siple Dome and Lago Guanaco records suggests that the westerly variations observed in SW Patagonia also affected the western Antarctic region of the Southern Ocean; taken together, these data suggest that the southern boundary of the westerlies may have extended farther south during the LIA. The simultaneous increase in wind intensity observed in both records indicates an overall increase in the atmospheric circulation in the southern high-latitudes during the LIA. In addition, our results are consistent with paleoclimate records compiled by Shulmeister et al. (2004) who also argue for an intensification of the westerlies during the LIA.

Although the covariance of west Antarctic and southwest Patagonian records can be attributed to a simple poleward shift of the westerly wind field, an alternative explanation for this agreement lies in the westerly intensification observed in both these locations during the positive phase of the Southern Annular Mode (SAM). The SAM is the major mode of atmospheric variability in the high southern latitudes and it is characterized by zonally symmetric geopotential height alterations between the polar ice cap and the mid-latitudes (Gillet et al., 2006). The positive phase of the SAM produces decreased geopotential height over Antarctica and increased geopotential height over the mid-latitudes, strengthening and shifting the high-latitude southern westerlies poleward and strengthening the polar vortex. The two paleoclimate records from Antarctica and SW Patagonia suggest that this mode of atmospheric circulation has been significant during the last 500 years.

6. Conclusions

The Lago Guanaco record provides a unique view of hydrologic change caused by variability in the Southern Hemisphere westerly wind field during the last millennium. This work allows us to draw three important conclusions as follows:

1. We identify significant changes in hydrology during the last 1200 years in SW Patagonia as interpreted from the $\delta^{18}O$ of biogenic carbonates and fine-fraction sediment. Century-scale periods of increased evaporation occur at ~800, 600, and 300 cal yr BP, while periods of reduced evaporation occur at the base of the record to 1000 cal yr BP and between 550 and 450 cal yr BP. We find evidence for drying during the MCA in the Guanaco record. This timing is consistent with other paleoclimate records from Patagonia.
2. When our $\delta^{18}O$ results are combined with pollen data from the lake, we identify the LIA as a period dominated by intense westerly flow, increased precipitation, and highly evaporative conditions. Lacustrine isotopic and palynological data, combined with evidence from Antarctic ice cores, indicate that the changes observed in SW Patagonia are regional rather than local and that the intensification of the westerlies during the LIA was accompanied by a poleward shift in the southern margin of the wind field.
3. We interpret four periods of increased lake productivity centered on 900, 650, 500, and 200 cal yr BP based on simultaneous increases in the $\delta^{13}C$ of bulk organic material and biogenic carbonate. Increased lake productivity is most likely related to increased summer temperatures, although changes in nutrient mixing in the water column related to changing wind velocities can also play a role. The 1–2‰ reduction in $\delta^{13}C$ in all four proxies in the uppermost 100 years of the Lago Guanaco is related to a combination of the

soil-derived DIC due to land use changes (deforestation) and the Suess effect.

Acknowledgments

This work was funded by a US State Department Fulbright to Chile, Department of Energy Global Change Education Program Graduate Fellowship, and a Stanford School of Earth Sciences McGee grant to C. Moy. R. Villa-Martínez and P.I. Moreno acknowledge Fondecyt Grants #1040204 and 1070991, National Geographic Society #7416-03, CEQUA, and the Institute of Ecology and Biodiversity (ICM P02-051). Radiocarbon analyses were performed under the auspices of the U.S. Department of Energy by the University of California, Lawrence Livermore National Laboratory under Contract No. W-7405-Eng-48. We would like to thank A. Schwalb for help in ostracode and bivalve identification, P. Brooks for analyzing the isotopic composition of the lake water, E. Sagredo, C. Díaz, J. Videla and M. Kaplan for field assistance, and J. Pardo and I. Ramírez (CONAF) for collecting water samples. In addition, we thank the CONAF administration of Parque Nacional Torres del Paine for their support and the Direccion General de Aguas (DGA) for the use of Torres del Paine meteorological data. Helpful discussions with K. Theissen and C. Neil Roberts improved the manuscript. We thank Ricardo Villalba and an anonymous reviewer for their helpful and insightful comments.

References

Aniya, M., 1995. Holocene glacial chronology in Patagonia: Tyndall and Upsala Glaciers. Arctic and Alpine Research 27 (4), 311–322.

Blindow, I., Dietrich, J., Mollmann, N., Schubert, H., 2003. Growth, photosynthesis and fertility of *Chara aspera* under different light and salinity conditions. Aquatic Botany 76, 213–234.

Bradley, R.S., Briffa, K.R., Cole, J., Hughes, M.K., Osborn, T.J., 2003. The climate of the last millennium. In: Alverson, K.D., Bradley, R.S., Pederson, T.F. (Eds.), Paleoclimate, Global Change and the Future. Springer, New York, pp. 105–141.

Brenner, M., Whitmore, T.J., Curtis, J.H., Hodell, D.A., Schelske, C.L., 1999. Stable isotope (d13C and d15N) signatures of sedimented organic matter as indicators of historic lake trophic state. Journal of Paleolimnology 22, 205–221.

Campos, H., Soto, D., Steffen, W., Parra, O., Aguero, G., Zuniga, L., 1994. Limnological studies of Lake Sarmiento (Chile): a subsaline lake from Chilean Patagonian. Archives of Hydrobiology 1–2, 217–234.

DeMaster, D.J., 1981. The supply and accumulation of silica in the marine environment. Geochimica et Cosmochimica Acta 45, 1715–1732.

Dettman, D.L., Reische, A.K., Lohmann, K.C., 1999. Controls on the stable isotope composition of seasonal growth bands in fresh-water bivalves (unionidae). Geochimica et Cosmochimica Acta 63, 1049–1057.

Garreaud, R., 2007. Precipitation and circulation covariability in the extratropics. Journal of Climate 20, 4789–4797.

Ghil, M.R., Allen, M., Dettinger, M.D., Ide, K., Kondrashov, D., Mann, M.E., Robertson, A., Saunders, A., Tian, Y., Varadi, F., Yiou, P., 2002. Advanced spectral methods for climatic time series. Reviews of Geophysics 40 (1), 3.1–3.41.

Gillet, N., Kell, T.D., Jones, P.D., 2006. Regional climate inpacts of the Southern Annular Mode. Geophysical Research Letters 33 (L23704).

Glasser, N.F., Harrison, S., Winchester, V., Aniya, M., 2004. Late Pleistocene and Holocene palaeoclimate and glacier fluctuations in Patagonia. Global and Planetary Change 43, 79–101.

Gruber, N., Keeling, C.D., Bacastow, R.B., Guenther, P.R., Lueker, T.J., Wahlen, M., Meijer, H.A.J., Mook, W.G., Stocker, T.F., 1999. Spatiotemporal patterns of carbon-13 in the global surface oceans and the oceanic Suess effect. Global Biogeochemical Cycles 13, 307–335.

Hammarlund, D., 1997. Multi-component carbon isotope evidence of early Holocene environmental change and carbon-flow pathways from a hard-water lake in northern Sweeden. Journal of Paleolimnology 18, 219–233.

Huber, U.M., Markgraf, V., 2003. European impact on fire regimes and vegetation dynamics at the steppe-forest ecotone of southern Patagonia. The Holocene 13, 567–579.

Huber, U.M., Markgraf, V., Schabitz, F., 2004. Geographical and temporal trends in Late Quaternary fire histories of Fuego-Patagonia, South America. Quaternary Science Reviews 23 (9–10), 1079–1097.

IAEA/WMO, 2004. Global Network of Isotopes in Precipitation. The GNIP Database.

Ito, E., 2001. Application of stable isotope techniques to inorganic and biogenic carbonates. In: Last, W.M., Smol, J.P. (Eds.), Tracking Environmental Change Using Lake Sediments. Kluwer Academic Publishers, Norwell, MA, pp. 351–371.

Kalnay, E., Kanamitsu, M., Kistler, R., Collins, W., Deaven, D., Gandin, L., Iredell, M., Saha, S., White, G., Woollen, J., Zhu, Y., Leetmaa, A., Reynolds, B., Chelliah, M., Ebisuzaki, W., Higgins, W., Janowiak, J., Mo, K., Ropelewski, C., Wang, J., Jenne, R., Joseph, D., 1996. The NCEP/NCAR 40-year re-analysis project. Bulletin of the American Meteorological Society 77, 437–471.

Kreutz, K.J., Mayewski, P.A., Meeker, L.D., Twickler, M.S., Whitlow, S.I., Pittalwala, I.I., 1997. Bipolar changes in atmospheric circulation during the little ice. Science 277, 1294–1296.

Le Quere, C., Rodenbeck, C., Buitenhuis, E.T., Conway, T.J., Langenfelds, R., Gomez, A., Labuschagne, C., Ramonet, M., Nakazawa, T., Metzl, N., Gillet, N., Heimann, M., 2007. Saturation of the Southern Ocean CO_2 sink due to recent climate change. Science 316, 1735–1738.

Leng, M.J., Marshall, J.D., 2004. Palaeoclimate interpretation of stable isotope data from lake sediment archives. Quaternary Science Reviews 23 (7–8), 811–831.

Li, H.-C., Ku, T.-L., 1997. $\delta^{13}C$–$\delta^{18}O$ covariance as a paleohydrological indicator for closed-basin lakes. Palaeogeography Palaeoclimatology Palaeoecology 133, 69–80.

Linacre, E., 1992. Climate Data and Resources: A Reference and Guide. Routledge, London.

Lorrain, A., Paulet, Y.M., Chauvaud, L., Dunbar, R., Mucciarone, D.A., Fontugne, M., 2004. $\delta^{13}C$ variation in scallop shells: increasing metabolic carbon contribution with body size? Geochimica et Cosmochimica Acta 68 (17), 3509–3519.

Martinic, M.B., 1964. Presencia de Chile en la Patagnia austral: 1843–1879. Universitaria, Santiago de Chile.

McConnaughey, T.A., 1991. Calcification in *Chara corallina*: CO_2 hydroxylation generates protons for bicarbonate assimilation. Limnology and Oceanography 36, 619–628.

McConnaughey, T.A., Burdett, J., Whelan, J.F., Paull, C.K., 1997. Carbon isotopes in biological carbonates: respiration and photosynthesis. Geochimica et Cosmochimica Acta 61 (3), 611–622.

McCormac, F.G., Hogg, A.G., Blackwell, P.G., Buck, C.E., Higham, T.F.G., Reimer, P.J., 2004. SHCal04 Southern Hemisphere calibration 0–11.0 cal kyr BP. Radiocarbon 46, 1087–1092.

Mercer, J.H., 1970. Variations of some Patagonian glaciers since the Late Glacial: II. American Journal of Science 269, 1–25.

Mercer, J.H., 1982. Holocene glacial variations in southern South America. Striae 18, 35–40.

Meyers, P.A., 1997. Organic geochemical proxies of paleoceanographic, paleolimnologic, and paleoclime processes. Organic Geochemistry 27 (5–6), 213–250.

Meyers, P.A., 2003. Applications of organic geochemistry to paleolimnological reconstructions: a summary of examples from the Laurentian Great Lakes. Organic Geochemistry 34, 261–289.

Meyers, P.A., Teranes, J.L., 2002. Sediment organic matter. In: Last, W.M. (Ed.), Tracking Environmental Change Using Lake Sediments. Volume 2: Physical and Geochemical Methods. Kluwer Academic Publishers, Hingham, MA, USA, pp. 239–270.

Mortlock, R.A., Froelich, P.N., 1989. A simple method for the rapid determination of biogenic opal in pelagic marine sediments. Deep-Sea Research, Part I (Oceanographic Research Papers) 36, 1415–1426.

O'Reilly, C.M., Alln, S.R., Plisnier, P.D., Cohen, A.S., McKee, B.A., 2003. Climate change decreases aquatic ecosystem productivity of Lake Tanganyika, Africa. Nature 424, 766–768.

Pentecost, A., Andrews, J.E., Dennis, P.F., Marca-Bell, A., Dennis, S., 2006. Charophyte growth in small temperate water bodies: extreme isotopic disequilibrium and implications for the palaeoecology of shallow marl lakes. Palaeogeography Palaeoclimatology Palaeoecology 240, 389–404.

Schelske, C.L., Hodell, D.A., 1995. Using carbon isotopes of bulk sedimentary organic matter to reconstruct the history of nutrient loading and eutrophication in Lake Eire. Limnology and Oceanography 40 (5), 918–929.

Schneider, C., Glaser, M., Kilian, R., Santana, A., Butorovic, N., G., C., 2003. Weather observations across the southern Andes at 53°S. Physical Geography 24, 97–119.

Schwalb, A., Burns, S.J., Cusminsky, G., Kelts, K., Markgraf, V., Team, P.L.D., 2002. Assemblege diversity and isotopic signals of modern ostracodes and host waters from Patagonia, Argentina. Palaeogeography Palaeoclimatology Palaeoecology 187, 323–340.

Seltzer, G.O., Rodbell, D.T., Burns, S.J., 2000. Isotopic evidence for late Quaternary climatic change in tropical South America. Geology 28 (1), 35–38.

Shulmeister, J., Goodwin, I., Renwick, J., Harle, K., Armand, L., McGlone, M.S., Cook, E., Dodson, J., Hesse, P.P., Mayewski, P., Curran, M., 2004. The Southern Hemisphere westerlies in the Australasian sector over the last glacial cycle: a synthesis. Quaternary International 118–119, 23–53.

Sigman, D.M., Boyle, E.A., 2000. Glacial/interglacial variations in atmospheric carbon dioxide. Nature 407, 859–869.

Stern, C.R., 2008. Holocene tephrochronology record of large explosive eruptions in the southernmost Patagonian Andes. Bulletin of Volcanology 70 (4), 435–454.

Stern, L.A., Blisniuk, P.M., 2002. Stable isotope composition of precipitation across the southern Patagonian Andes. Journal of Geophysical Research 107 (D23), 3-1–3-14.

Stine, S., 1994. Extreme and persistent drought in California and Patagonia during mediaeval time. Nature 369, 546–549.

Stuiver, M., Reimer, P.J., 1993. Extended ^{14}C database and revised CALIB radiocarbon calibration program (version 5). Radiocarbon 35, 215–230.

Talbot, M.R., 1990. A review of the palaeohydrological interpretation of carbon and oxygen isotopic ratios in primary lacustine carbonates. Chemical Geology 80, 261–279.

Toggweiler, J.R., Russell, J.L., Carson, S.R., 2006. Midlatitude westerlies, atmospheric CO_2, and climate change during the ice ages. Paleoceanography 21, PA2005.

Trenberth, K.E., 1991. Storm tracks in the Southern Hemisphere. Journal of the Atmospheric Sciences 48 (19), 2159–2178.
Verardo, D.J., Froelich, P.N., McIntyre, A., 1990. Determination of organic carbon and nitrogen in marine sediments using the Carlo Erba NA-1500. Deep-Sea Research, Part I (Oceanographic Research Papers) 37, 157–165.
Villalba, R., 1994. Tree-ring and glacial evidence for the Medieval Warm Epoch and the Little Ice Age in southern South America. Climatic Change 26 (2–3), 183–197.
Villalba, R., Lara, A., Boninsegna, J.A., Masiokas, M., Delgado, S., Aravena, J.C., Roig, F.A., Schmelter, A., Wolodarsky, A., Ripalta, A., 2003. Large-scale temperature changes across the southern Andes: 20th-century variations in the context of the past 400 years. Climatic Change 59 (1–2), 177–232.
Villa-Martinez, R., Moreno, P.I., 2007. Pollen evidence for variations in the southern margin of the westerly winds in SW Patagonia over the last 12,600 years. Quaternary Research 68 (3), 400–409.
von Grafenstein, U., Erlenkeuser, H., Trimborn, P., 1999. Oxygen and carbon isotopes in modern fresh-water ostracod valves: assessing vital offsets and autoecological effects of interest for paleoclimate studies. Palaeogeography Palaeoclimatology Palaeoecology 148, 133–152.
Winn, R.D., Dott, R.H., 1979. Deep-water fan-channel conglomerates of Late Cretaceous age, southern Chile. Sedimentology 26, 203–228.
Wollheim, W.M., Lovvorn, J.R., 1996. Effects of macrophyte growth forms on invertebrate communities in saline lakes of the Wyoming High Plains. Hydrobiologia 323, 83–96.